

Review

Polymeric Bioinks for 3D Hepatic Printing

Joyita Sarkar ^{1,*}, Swapnil C. Kamble ^{2,*}  and Nilambari C. Kashikar ² 

¹ Institute of Chemical Technology, Mumbai, Marathwada Campus Jalna, BT-6/7, Biotechnology Park, Additional MIDC Area, Aurangabad Road, Jalna 431203, Maharashtra, India

² Department of Technology, Savitribai Phule Pune University, Ganeshkhind, Pune 411007, Maharashtra, India; kashikarnilambari13@gmail.com

* Correspondence: j.sarkar@marj.ictmumbai.edu.in (J.S.); sckamble@unipune.ac.in (S.C.K.)

Abstract: Three-dimensional (3D) printing techniques have revolutionized the field of tissue engineering. This is especially favorable to construct intricate tissues such as liver, as 3D printing allows for the precise delivery of biomaterials, cells and bioactive molecules in complex geometries. Bioinks made of polymers, of both natural and synthetic origin, have been very beneficial to printing soft tissues such as liver. Using polymeric bioinks, 3D hepatic structures are printed with or without cells and biomolecules, and have been used for different tissue engineering applications. In this review, with the introduction to basic 3D printing techniques, we discuss different natural and synthetic polymers including decellularized matrices that have been employed for the 3D bioprinting of hepatic structures. Finally, we focus on recent advances in polymeric bioinks for 3D hepatic printing and their applications. The studies indicate that much work has been devoted to improvising the design, stability and longevity of the printed structures. Others focus on the printing of tissue engineered hepatic structures for applications in drug screening, regenerative medicine and disease models. More attention must now be diverted to developing personalized structures and stem cell differentiation to hepatic lineage.

Keywords: 3D bioprinting; polymeric bioinks; hepatic tissue engineering



Citation: Sarkar, J.; Kamble, S.C.; Kashikar, N.C. Polymeric Bioinks for 3D Hepatic Printing. *Chemistry* **2021**, *3*, 164–181. <https://doi.org/10.3390/chemistry3010014>

Received: 4 December 2020

Accepted: 26 January 2021

Published: 1 February 2021

Publisher's Note: MDPI stays neutral with regard to jurisdictional claims in published maps and institutional affiliations.



Copyright: © 2021 by the authors. Licensee MDPI, Basel, Switzerland. This article is an open access article distributed under the terms and conditions of the Creative Commons Attribution (CC BY) license (<https://creativecommons.org/licenses/by/4.0/>).

1. Introduction

The liver is an important organ that performs synthetic (albumin and bile components), detoxification (ammonia removal from blood) and metabolic (xenobiotics and lipids) functions [1,2]. It is also a complicated organ containing parenchymal (hepatocytes) and non-parenchymal cells that comprise other cell types of liver. Hepatocytes are differentiated epithelial cells that perform most of the liver functions. The non-parenchymal cells constitute liver sinusoidal endothelial cells which scavenge wastes, hepatic stellate cells that produce extracellular matrix (ECM) components such as collagen, kupffer cells exhibiting phagocytic activity, cholangiocytes involved in the secretion of bile components and hepatic progenitor cells which are small and quiescent stem cells with bi-potential differentiation capacity into hepatocytes and cholangiocytes [3–7]. The cells of liver exhibit both homotypic and heterotypic cell–cell and cell–ECM interactions. The hepatocytes extensively interact with each other via gap junctions, tight junctions, intermediate junctions and desmosomes. The interaction of hepatocytes with other non-parenchymal cells plays an important role in maintaining normal liver function. These interactions are mainly mediated by paracrine signaling. The ECM controls the expression of differentiated phenotypes of hepatocytes and non-parenchymal cells. The ECM components are crucial for cell adhesion and architecture as well as for maintenance of cytoskeletal structure [3,7]. In the case of diseased liver, the ECM becomes stiffer from the normal to cirrhotic stage; the same acts a marker for the progression of liver disease [8]. Liver diseases are either hereditary or acquired; the latter is classified as hyper-acute, acute and sub-acute based on the time of occurrence with 10 days, 10–31 days and more than 31 days, respectively [9]. Chronic liver failure occurs

due to end-stage cirrhosis and is associated with massive tissue damage. Acute-on-chronic liver disease occurs when there is already a chronic liver disease upon which an acute liver collapse occurs. Of the many reasons for liver injury and failure, among the leading causes is drug-induced liver injury that can imitate different acute and chronic liver conditions and infections. Drug-induced liver injury is either non-idiosyncratic (i.e., predictable) and dose dependent or idiosyncratic (i.e., unpredictable), which mainly arise due to host risk factors such as genetic variations in drug metabolizing enzymes, environmental factors such as increased vulnerability due to an existing disease or drug–drug interactions when co-administered with other drugs. It is also a major reason for drug attrition, especially at later stages [10,11]. Liver is vital for studying the toxicity and metabolic profile of drugs and other xenobiotic compounds. On the other hand, limited regeneration capacity in some cases has also led to the development of bioartificial liver devices. Both the fields demand the huge involvement of tissue engineering strategies that in turn is being largely impacted by three-dimensional (3D) printing technologies.

First established by Charles W. Hull in 1986, 3D printing has now become indispensable for tissue engineering applications due to its ability to construct structures with complicated geometries and patterns inherent to tissues *in vivo* [12]. Bioprinting can be defined as a 3D printing process that simultaneously prints cells together with cell-compatible materials (e.g., polymers) and curing processes (e.g., photocrosslinking). Biomaterials, cells and bioactive molecules can be precisely delivered to desired designs and locations to fabricate living and functional tissue constructs [13]. The complexity imposed by multiple cells, ECM components, diverse functions and pathologic conditions poses a challenge to resemble a physiologically relevant liver tissue, and 3D bioprinting techniques hold promising attributes for developing complex tissues. Three-dimensional printed hepatic structures are tunable and capable of providing long-term viability, functionality and mechanical stability. This is indeed very important for hepatic tissue engineering applications that require models for *in vivo* drug screening, *ex situ* bioartificial liver support and *in vivo* implantation applications that enable the development of personalized medicines and treatment regimes, along with regenerative medicine strategies [14–16]. In this review, we emphasize the use of cell laden polymeric bioinks in 3D hepatic printing. Focus is drawn to the recent advances in bioprinting of the liver after a brief introduction to printing techniques and different polymers, both natural and synthetic used for the purpose. We selected recent publications with emphasis on the last 5 years. Key words used to search were “3D printing”, “liver”, “hepatic decellularized extracellular matrix”, “bioink”, “bioprinted liver”, “polymeric bioink”, “polymers”, “hepatic printing”, “hepatic 3D printing”, either standalone or in combination. In addition, searches for studies of 3D hepatic bioprinting for individual polymers such as gelatin, alginate, agarose and/or cellulose were also conducted.

2. 3D Printing and Its Prerequisites

Three-dimensional printing, additive manufacturing or rapid prototyping refer to several manufacturing technologies that generate a physical model from digital information. Three-dimensional printing enables the fabrication of complex forms with high precision, through a layer-by-layer addition of different materials. Expectedly, 3D printing has emerged as the next generation of fabrication technique and has spanned across various research areas. The 3D printing technology represents a big opportunity for pharmaceutical and medical companies to create personalized drugs by providing screening platforms and enabling a rapid production of medical implants. Three-dimensional printing has gained considerable attention in the medical field with the objective to produce scaffolds to repair or replace damaged tissues and organs [17]. A typical 3D printing system contains different parts as illustrated in Figure 1A. Some of them are described below:

1. Filament—a filament-shaped polymer of required material, in which a 3D model is printed.
2. Extruder motor—has a heating coil which melts the filament for printing.

- Hot end—the end of the extruder motor which extrudes melted polymer on a heating bed. It is connected to the X- and Z-axis motor to print in the X- and Z-axis.
- Heated bed—a platform on which the 3D model is printed. It is connected to the Y-axis motor to move the platform in the Y-axis.
- Programmable Logic Control (PLC) and computer input—gives input to the PLC. The PLC reads that input and performs actions as per the given commands.

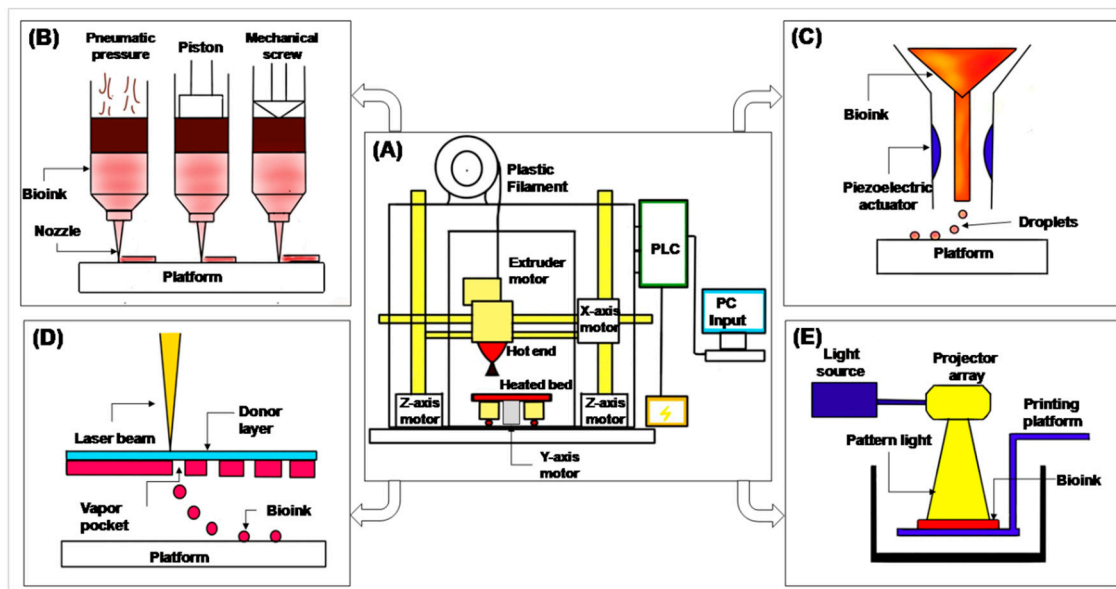


Figure 1. Schematic showing different 3D printing techniques. (A) General 3D printing apparatus. (B) Extrusion printer. (C) Inkjet printer. (D) Laser assisted printer. (E) Stereolithographic printer.

The different types of 3D printing techniques can be broadly classified into extrusion bioprinting, inkjet printing, laser assisted printing and stereolithographic printing. Extrusion bioprinting is the most widely used 3D printing method. The plunger, when applied with a continuous force, can extrude uninterrupted cylindrical lines rather than discrete droplets (Figure 1B). It provides compatibility for highly viscous materials. It can print various materials simultaneously at a reasonable cost for almost all bioinks. The main advantage of this method is its ability to make large 3D structures with the use of any viscous material. During the process, cell viability may be hampered due to high mechanical stress [18–21]. Inkjet printing is the first bioprinting technique used for organ printing. The production material contains a mixture of hydrogel pre-polymer solution and cells (i.e., bioink) [18,22–26]. The printing of hydrogel and bioink depends on the piezoelectric transducer which allows the printer head to squeeze out the printing materials (Figure 1C). The printing provides high cell viability at a low cost. It cannot print viscous polymers and may produce clogging and non-uniformity in cell concentration at the printing interval.

The principle of laser assisted printing is laser-induced transfer technology, which is a modified version of inkjet bioprinting. The step-up contains three layers of an energy-absorbing donor layer that responds to laser stimulation, a bioink layer underneath the donor layer and a collecting layer to form tissue constructs (Figure 1D). A laser pulse is focused on a small area of the top donor layer. Upon energy absorption, this small area in the donor layer vaporizes and creates a high-pressure air bubble at the interface between the donor and bioink layers. The air bubble propels the suspended bioink to form a droplet that is eventually received by the bottom collecting layer. It can print highly viscous materials with high cell density. However, the printing cost is high because of pulse laser generator and non-reusable donor layer. It is difficult to build large 3D scaffolds by this method [18,22,27]. Stereolithographic printing is the latest technique used for light sensitive bioink, and is a light-based printing technique. During stereolithographic bioprinting, a patterned binary image from a projector is used to cure a layer of photocurable bioink

(Figure 1E). Only the areas exposed to high-intensity white light receive sufficient energy to cure. In this way, a layer of solid tissue construct is formed. The advantage of this rapid technique is that it provides the highest spatial resolution. However, it cannot print multiple materials simultaneously [18,28,29].

Regardless of the source of the polymer, there are certain criteria that must be satisfied for a polymer to be utilized for bioprinting. The most important is of course the biocompatibility of the polymer that holds for all types of biomaterials. The polymer must be non-toxic to the cell whether or not it allows for adherence of the cell. In conditions where the cells are bioprinted along with the polymer, it might be desirable that the polymer is cytoadherent so as to provide structural support and surface for the proliferation and/or expansion of the cells [30–32]. However, this has not limited the use of non-cytoadherent polymers in cell bioprinting, but they have been surface modified on multiple occasions to provide adherence site to the cells [30,31,33]. The next important property is the printability of the polymer, which is largely affected by the viscoelastic or rheological properties of the polymer solution that in turn may depend on the concentration of the polymer in the solution as well as the solvent. Different printing methods require polymer solutions with different viscoelastic properties [32,34]. In general terms, a polymer solution with a high viscosity is expected to yield more stable printed structures. However, high viscous solutions are difficult to impel out of the printing nozzle, thereby requiring more pressure, which may lead to clogging of the nozzle. Additionally, the stress between the bioink and wall of the nozzle can disrupt the cell membrane in the case of cell laden bioinks [34]. This can be overcome by the shear thinning of the polymer solution during which the viscosity of the polymer solution is reduced due to the shear stress it experiences while passing through the small nozzle, ultimately easing the passage of the viscous polymer ink [35,36]. Another important property of the polymer bioink is its degradation chemistry as well as the stiffness of the printed structure. Both should preferably match the characteristics of the tissue in concern [35–37]. Biodegradability is concerned with the restoration of the tissue functions, while the stiffness is associated with multiple cellular activities such as proliferation and differentiation, thereby contributing to the regeneration of the concerned tissue [38–41].

3. Polymers Used as Bioinks in 3D Hepatic Printing

Polymers are large chains constituting repeating units of monomer linked by covalent bonds. Based on their origin, polymers are either natural or synthetic [42]. The natural polymers are abundant in plant and animal extracellular matrices and so have much similarity to the extracellular matrix of tissues/organs and, therefore, justify most of the prerequisites of biomaterials. They are biocompatible, biodegradable, non-toxic, retain moisture and support angiogenesis, neurogenesis, lymphogenesis, organogenesis and tissue/organ maturation under specific physiological conditions. Many of the natural polymers are water soluble as well. Synthetic polymers, as the name suggests, are man-made and synthesized under predefined conditions that greatly affect their properties. The main advantage of synthetic polymers is that they provide an opportunity to design as per the requirement of the application, for example, mimicking certain features of tissues/organs. They also allow tailoring and tuning of the physicochemical properties of the biomaterial such as the mechanical properties and surface properties by controlled chemical modifications. These advantages are imparted due to tunable synthesis conditions of the polymers that proffer control over the chain length, molecular weight, branching, geometry and distribution of the monomers, thereby imparting desired properties to the polymer [30,43,44]. The general properties of different polymers are summarized in Table 1.

Table 1. Major properties of different polymers used as bioinks for 3D bioprinting of hepatic structures.

Polymer	Biomolecule Class	Cytoadherent	Aqueous Solubility	Biodegradable	Other Important Properties	References
Natural Polymers						
Gelatin	Protein/Peptide	Yes	Soluble	Yes	Self-gelation at lower temperatures	[30,31,45–53]
Alginate	Polysaccharide	No	Soluble	Yes	Cationic gelation	[15,30,31,44,53–59]
Agarose	Polysaccharide	No	Soluble at high temperature	Yes	Provides exceptional mechanical support	[30,31,37,44,60,61]
Collagen	Protein	Yes	Soluble at low pH	Yes	High gelation time at 37 °C	[30,31,44,62–65]
Cellulose	Polysaccharide	No	Insoluble	No	Efficient for long-term application	[30,31,44,66–69]
Chitosan	Polysaccharide	No	Soluble at low pH	Yes	Poor gelation and mechanical strength	
Synthetic Polymers						
PEG ¹	Polyether	No	Soluble	No	Effective control on mechanical strength	[30]
PCL ²	Polyester	No	Insoluble	Yes	Produces stiff structures	[30]
PLGA ³	Polyester	No	Degrades in water	Yes	–	[30]
Decellularized Matrix						
Liver dECM ⁴	Proteins, polysaccharide, glycoproteins, proteoglycans	Yes	Soluble	Yes	Retains native chemical structure and microgeometry	[30,70,71]

¹ PEG: poly(ethylene oxide); ² PCL: polycaprolactone; ³ PLGA: poly(lactic-co-glycolic acid); ⁴ dECM: decellularized extracellular matrix.

3.1. Natural Polymers

Natural polymers are the preferred choice for engineering soft tissues owing to their properties. Therefore, they have been largely used for bioprinting of the liver which is an organ of stiffness approximately 1.5–2 kPa. Of the many natural polymers, gelatin and alginate have been extensively used for 3D hepatic bioprinting. Gelatin, a single chain polymer, is derived from partial hydrolysis and breaking of the triple helix structure of collagen extracted from tissues of different animals, for example, fish, bovine or porcine (Figure 2A). Gelatin is highly soluble in biological buffers and cell culture media, enabling the preparation of cell and bioactive agent laden bioink for 3D printing. Thermosensitivity is also exhibited by the sol–gel transition of gelatin at a temperature range of 20–35 °C. The polymer is also highly biocompatible, cytoadherent and non-immunogenic. Gelatin is completely non-toxic to all types of cells and elicits no adverse immune response such as cytokine activation, inflammation, etc. when administered in vivo [30,31]. It also contains the tripeptide motif, Arg-Gly-Asp, which is recognized by integrins on the cell membrane for attachment. Colosi et al. were able to exhibit excellent adhesion of HUVEC cells on a gelatin-based microfluidic bioprinted tissue construct (Figure 3A) [45]. Wang et al. and Gaetani et al. also showed improved adherence of liver and cardiac progenitor cells on gelatin-based hydrogel and bioprinted patch, respectively [46,47]. Gelatin is biodegradable and printable, which makes it an excellent polymer for bioink. Xiao et al. demonstrated greater than 80% collagenase-mediated degradation of gelatin-based hydrogels [48]. The printability of gelatin solution is determined by the viscosity, which in turn depends on the polymer concentration and other additives to the solution that could be cells, bioactive agents, any other biomaterial (for blends and composites), etc. A highly viscous bioink was fabricated by Kang et al., comprising a composite of gelatin, hyaluronic acid, fibrinogen, glycerol and cells for bioprinting of human-scale tissues [49]. Lower gelatin concentration exhibits better cell viability though reduced stability of the printed structure. Post-printing, the stability of the construct depends both on the physical gelation and chemical crosslinking employed [50].

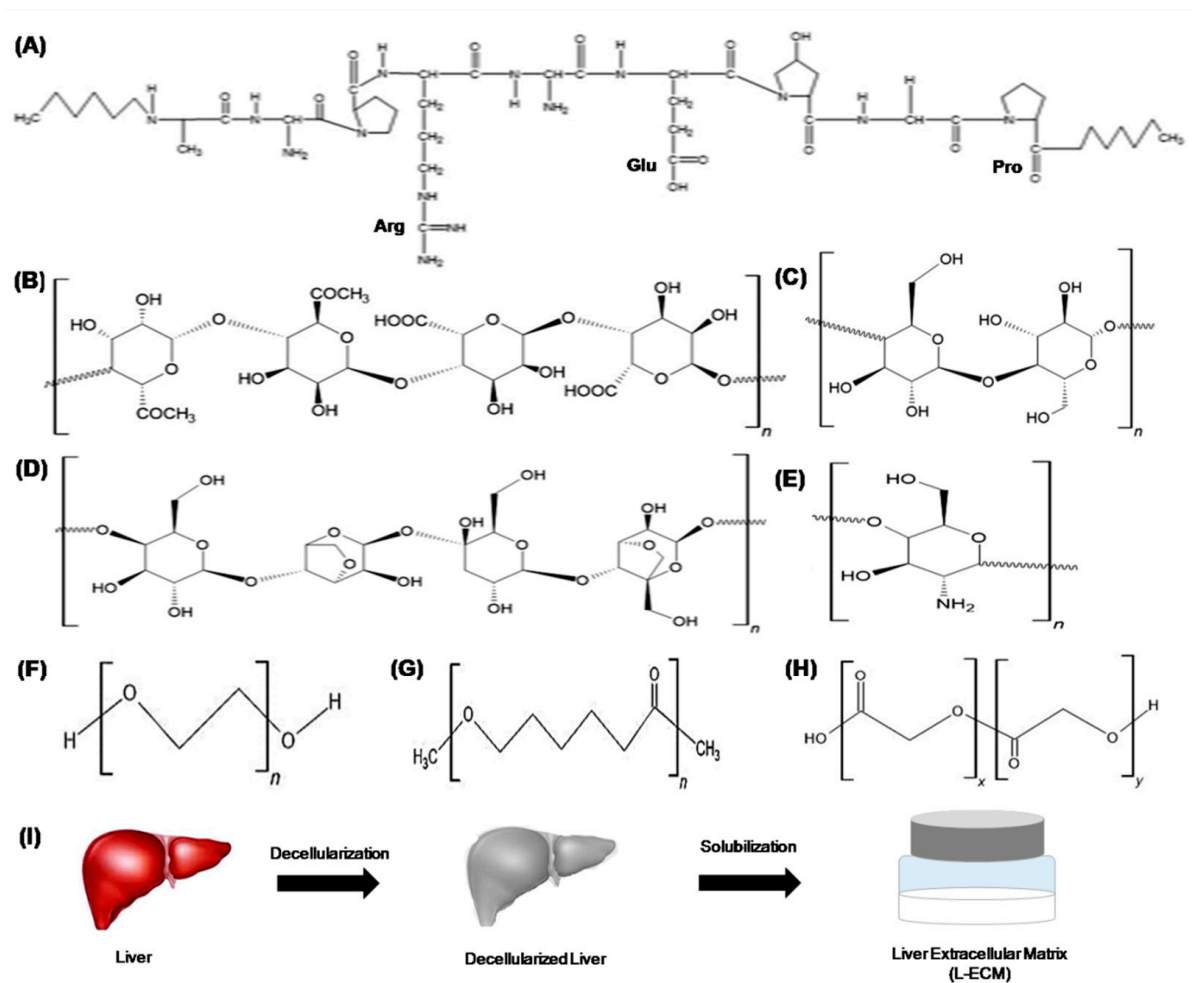


Figure 2. Schematic showing structure of different polymers used as bioinks. (A) Gelatin, (B) alginate, (C) cellulose, (D) agarose, (E) chitosan, (F) polyethylene glycol, (G) polycaprolactone, (H) poly(lactic-co-glycolic acid), (I) decellularized matrix (n —repeating unit of polymer; x —first repeating unit and y —second repeating unit of same polymer). All figures were drawn in software ACD/Chemsketch (freeware), Toronto, ON, Canada, Version 2020 1.2.

Gelatin is capable of self-gelation at lower temperatures by weak physical crosslinking but generates structures of poor strength when printed. To stabilize the printed structures, several chemical crosslinking methods are also employed; one of the most common instances is crosslinking by glutaraldehyde via Schiff's base formation with amino acid side chains of gelatin. An optimum gelatin concentration and crosslinking method will provide a bioprinted hepatic construct with desired mechanical strength and biocompatibility [51,52]. Apart from crosslinking by physical and chemical methods, photocrosslinking has also been achieved by methacryloylation of gelatin engendering gelatin methacrylate (GelMA). The methacryloyl groups are introduced in the amine and hydroxyl groups of amino acid side chains of gelatin. Crosslinking of GelMA can be achieved by adding a water-soluble photoinitiator followed by exposure to UV irradiation. The most commonly used photoinitiators include 2-hydroxy-1-[4-(2-hydroxyethoxy)phenyl]-2-methyl-1-propanone (Irgacure 2959), which has an aqueous solubility of 5 mg/mL [53]. The stiffness and cell viability of the bioprinted GelMA structure highly depends on the concentration of polymer, photoinitiator concentration and intensity of UV light. A study revealed that lower UV intensities exhibited better cell viability at both low and high concentrations of photoinitiator; however, the printed structures had low stiffness as well. This implies that exposure time of UV light can also be manipulated for obtaining a construct with optimum properties [72].

Alginate, algin or alginic acid is a natural, negatively charged or anionic polysaccharide obtained from brown seaweed algae. The polymer is composed of (1-4)- β -D-

mannuronic acid (M block) and α -L-glucuronic acid (G block), which are involved in gelation and imparting flexibility to the material, respectively (Figure 2B) [15,30,31]. Similar to gelatin, alginate is also highly soluble in water, but its sol–gel transition temperature is below 0 °C, which rules out any probability of physical gelation when printing at room or physiological temperature [44]. However, alginate can be ionically crosslinked by divalent cations such as Ca^{2+} by chelating with the carboxylate groups of the polymer, both intra and inter chain; the property is employed to impart stability to the bioprinted structures. Park et al. fabricated a hybrid bioink of low and high molecular weight alginate by cationic crosslinking using CaCl_2 (Figure 3B) [73]. The biocompatibility of alginate is inferior to that of gelatin; however, it does not elicit adverse immunological reactions when it is administered in vivo [30,31]. Apart from this, alginate is also biodegradable and non-cytoadherent. The stability of the post-printed structures largely depends on the degree of crosslinking by the divalent cation but is very susceptible to pH of the environment that can interrupt the ionic interaction between the polymer and ion. In usual practice, the alginate solution is first laden with cell and/or bioactive molecules, printed and then applied with the crosslinking cations either by spraying with or soaking in Ca^{2+} solution. Since the cations exhibit leaching out from the construct over time, the crosslinking is reversible, and the construct requires repeated treatment with the cation for long-term functionality. Similar to gelatin, the functionality of the alginate bioprinted structure depends on polymer concentration, cell density and degree of crosslinking [54–57]. Alginate has been successfully used for the bioprinting of many different tissues, for example, liver, heart, bone and cartilage. The cytoadherence was improved by incorporating adherent motifs such as Arg-Gly-Asp [58,59]. Agarose is another linear polysaccharide derived from marine source, red seaweed algae. It is composed of repeated agarobiose, which is a block of β -D-galactopyranose and 3,6-anhydro- α -L-galactopyranose (Figure 2C) [30,31]. It provides exceptional mechanical support to the structure and has a gelling temperature of approximately 30–45 °C. Fan et al. developed a hybrid bioink of Matrigel and agarose. Agarose was solely added to improve the printability of the ink and enhance the mechanical properties of the printed structures [37]. The gelation temperature, however, depends on the concentration of the polymer [44]. Agarose is highly biocompatible but is non-cytoadherent [60,61].

Another important natural polymer is collagen, which is the main component of all tissue ECM that renders it highly biocompatible and cytoadherent. Like gelatin, collagen also contains the Arg-Gly-Asp motif that supports cell adhesion, proliferation, migration and differentiation [3,31,44]. The incorporation of collagen in bioink has been shown to enhance angiogenesis and vascularization of the bioprinted structure (Figure 3C) [62,63]. Collagen can be crosslinked by change in pH, temperature and by adding chemical crosslinkers, but the gelation time at physiological temperature is quite high (around 30 min) [64]. Moreover, collagen is highly biodegradable especially in vivo [65]. This might pose a limitation to the use of collagen for 3D bioprinting applications. Cellulose, a linear polysaccharide, is also used as bioink in two different forms (Figure 2D) [30,31,44]. First is carboxymethyl cellulose that has very tunable properties depending on its degree of methylation and forms gel below physiological temperature [66]. Second is nanocellulose, which is basically nano-structured cellulose either in the form of crystal or fibers. Nanocellulose has been extensively and successfully used to bioprint structures for cartilage regeneration (Figure 3D) [67,68]. Like agarose, cellulose is biocompatible but non-cytoadherent. Additionally, cellulose is non-biodegradable, which makes it efficient for long-term application [69]. Another important polymer used in 3D bioprinting of the liver is chitosan. Chitosan is a polysaccharide obtained by deacetylation of chitin derived from crustacean shells (Figure 2E). It is biocompatible, non-cytoadherent, biodegradable and has antibiotic properties. However, inadequate mechanical properties (e.g., brittle) and gelation ability restrict its use in 3D printing [31].

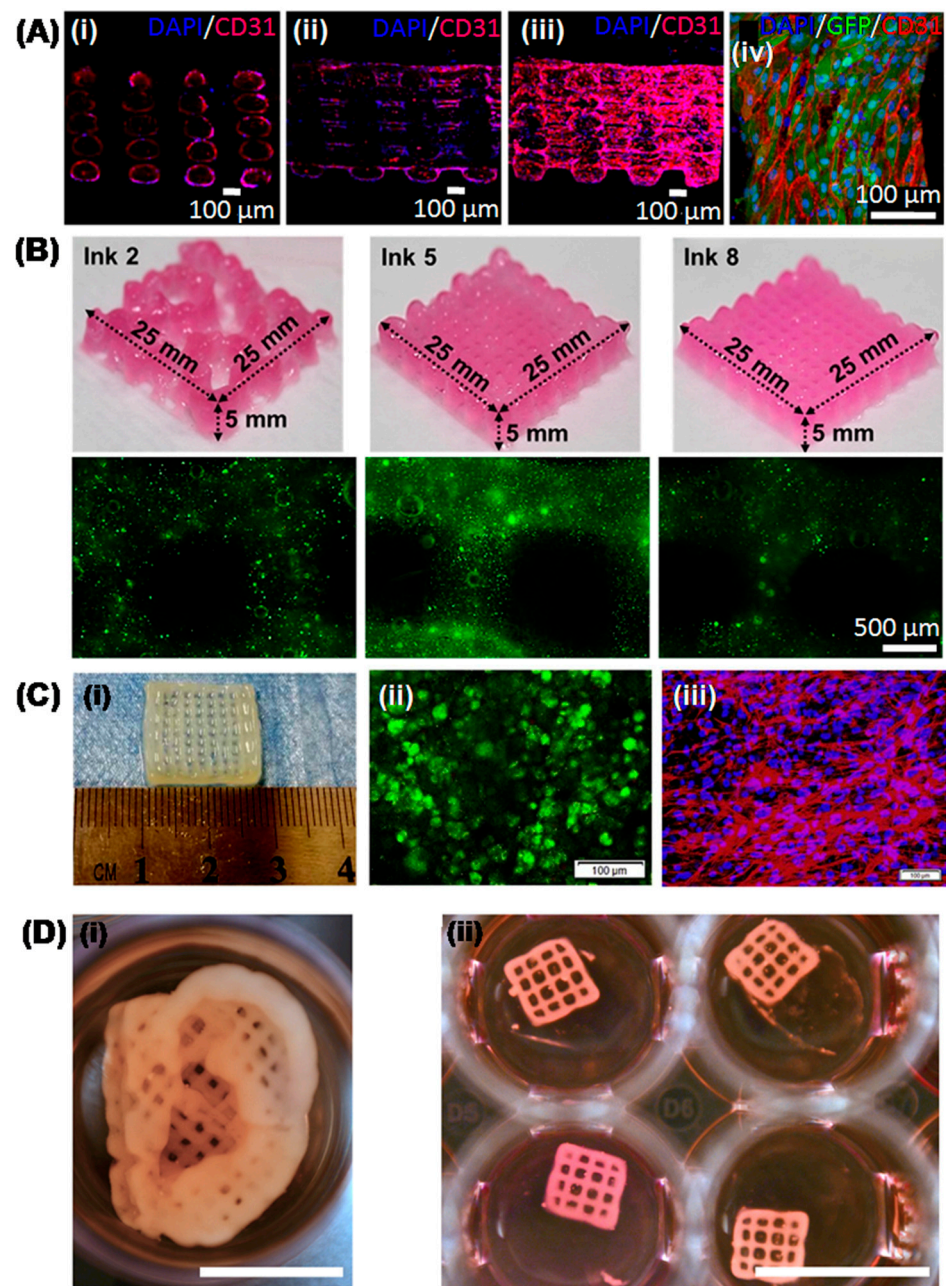


Figure 3. Three-dimensional bioprinted tissue constructs using polymeric bioinks. (A) Confocal microscopy images of a 1 mm thick bioprinted HUVEC construct using gelatin-based bioink. (i) transversal cross-section, (ii) longitudinal cross-section, (iii) outer surface of the complete construct. (iv) Top view of a single fiber immunostained for CD31 (red) and DAPI (blue). Scale bar: 100 μm ; GFP: Green fluorescent protein. Image reproduced with permission from [45]. (B) Upper panel: digital image of 3D bioprinted structures using alginate-based inks. Lower panel: fluorescence images of WST-1 cells printed in the alginate-based bioinks after 7 days of culture. Scale bar: 500 μm ; green: live cells. Image reproduced with permission from [73]. (C) Three-dimensional bioprinted structure using collagen-alginate bioink. (i) Digital image. (ii) Fluorescent image showing viability of bioprinted rat primary chondrocytes by Calcein-AM staining. (iii) Fluorescent image showing cytoskeleton morphology of bioprinted rat primary chondrocytes by rhodamine-phalloidin (Red)/Hoechst 33,258 (Blue) staining. Scale bar: 100 μm . Image reproduced with permission from [63]. (D) Three-dimensional bioprinted structure using nanofibrillated cellulose-based bioink. (i) Auricular and (ii) lattice structured construct with human nasal chondrocytes after 21 days of culture. Scale bar: 1 mm. Image reproduced with permission from [67].

3.2. Synthetic Polymers

Of many 3D printable synthetic polymers, polyethylene glycol (PEG), polycaprolactone (PCL) and poly(lactic-co-glycolic acid) (PLGA) are mainly used for bioprinting hepatic structures. While PEG hydrogels exhibit high water retention capacity similar to soft tissues such as liver, PCL and PLGA, they have very tunable mechanical properties and hence have been used to engineer both hard (e.g., bone) and soft (e.g., liver) tissues. The most commonly used synthetic polymer for bioprinting of the liver is probably PEG, also known as poly(ethylene oxide) (PEO) (Figure 2F). PEG is a United States-Food and Drug Administration (FDA)-approved polymer with excellent solubility in water. It is also biocompatible and non-immunogenic; though non-cytoadherent. The terminal hydroxyl groups of PEG can be chemically modified into acrylate, carboxylate and/or thiol to enable crosslinking of the polymer. The mechanical strength can be effectively controlled by degree of crosslinking. The viscosity of PEG solution solely depends on its molecular weight; however, high viscosity cannot be achieved by PEG solutions to be used in extrusion-based printing and inkjet printing [30]. Another popular synthetic polymer is PCL, which is non-toxic, biocompatible, hydrophobic, non-cytoadherent and exhibits slow biodegradation (Figure 2G). However, PCL is not soluble in water and requires organic solvents such as chloroform, benzene and toluene to dissolve, restricting its use in the direct printing of cell laden structures. Moreover, the stiffness of the structures is relatively high, which might not be suitable for the liver [30,44]. Apart from these, PLGA, a linear polyester of lactic acid and glycolic acid, has also been employed for the 3D printing of hepatic structures (Figure 2H). PLGA is also a US-FDA-approved polymer with commendable biocompatibility and biodegradability. The degradability of the polymer can be tailored by manipulating the content of lactic and glycolic acid in the copolymer; the higher the ratio of glycolic acid, the lower the degradation time. However, PLGA undergoes rapid hydrolysis of its ester bonds in water that limits the use of water as a solvent for PLGA. This restricts, similar to PCL, the printing of cell laden constructs with PLGA [30].

3.3. Decellularized Matrix

The decellularized liver matrix is a mixture of natural biopolymers and bioactive molecules obtained by chemical and/or enzymatic decellularization of the liver. The dried and decellularized ECM (dECM) thus obtained can be powdered and dissolved in biological buffers or media for the printing of cell laden structures (Figure 2I). The native chemical composition, microgeometry and biomolecules such as growth factors of the liver can be preserved by decellularization, which can provide an *in vivo*-like environment to the hepatic cells *in vitro*. Usually, dECM forms gel at physiological pH and temperature, which encourages its use in 3D printing; however, low viscosity of dECM solutions also poses restrictions. The ECM of the liver comprises only a 3% area of liver that constitutes Glisson's capsule, central veins, portal tracts and sinusoid walls [74–77]. The most abundant component of the liver ECM is collagen IV with type I, III and V also being present. Other than this, glycoproteins (fibronectin, laminin, etc.) and proteoglycans (heparin, hyaluronic acid, chondroitin sulphate, etc.) are also the major constituents of the liver ECM [70]. Though liver dECM provides an excellent candidate for bioink, the poor shape retention properties and rapid biodegradation limit its use for printing large structures and long-term use, respectively. Moreover, the most common source of dECM is xenogenic, especially porcine, which may pose immunogenic threat among *in vivo* introductions. Further, residual cellular structures may also elicit immunogenic reaction and can also alter cell fate [30,71]. Nevertheless, decellularized liver matrices have proved to be an excellent candidate as a bioink to print cell laden 3D hepatic structures.

4. Recent Advances in 3D Printed Hepatic Structures with Polymeric Bioink

It can be deduced from the previous section that none of the polymers possess all the adequate properties to yield a bioink comprising all the desired properties, such as cytoadherence and mechanical stability. Therefore, the majority of the studies on 3D hepatic

printing have utilized a blend/composite of different polymers and components as bioink to engender the required properties. An “at a glance” summary of the major studies on 3D hepatic bioprinting published in the last 5 years is presented in Table 2. Many approaches have been employed to improvise the printability of bioinks and the integrity of the bioprinted hepatic structures. In one such recent study by Kang and colleagues [34], dECM powder-based bioink (dECMpBio-ink) was prepared by mixing porcine dECM microparticles in gelatin containing hyaluronic acid and fibrinogen and bioactive components. The dECMpBio-ink exhibited higher viscosity, shear thinning and even distribution of ECM microparticles. A high aspect ratio was also obtained, exhibiting the 3D printability of the bioink. Furthermore, the novel ink was also cytocompatible with human liver and endothelial cells, thereby showing potential for multicellular liver construct. In another recent study by Gori et al. [78], thermoresponsive and bioinert semisynthetic alginate-pluronic ink was used to print hepatic structures with high shape fidelity imparted by a sacrificial pluronic template and control of gelation by thermoresponsive nature. The resultant hepatic structure exhibited enhanced hepatic functionalities and sensitivity towards acetaminophen, thereby showing more physiologically relevant properties. In another study by Lewis et al. [79], the uniformity of the specific geometrical architecture and pore size of the gelatin bioink printed structure with different strut spacing and angles was taken into consideration (Figure 4A). The structure though could not exhibit arrest in proliferation of Huh7 cells, as differentiated hepatocytes, but exhibited enhanced hepatic functionalities, such as albumin secretion and MRP2 protein expression [79]. In an interesting approach by Cho and colleagues [80], a bioink was prepared using liver dECM, and structures with high fidelity were printed. The construct exhibited differentiation of mesenchymal stem cells (MSCs) to hepatic lineage and also exhibited better functionality of human hepatocellular carcinoma, HepG2 cells as compared to commercially available collagen bioinks. The study was ingenious as it used solely dECM as a component of bioink and printed stable and functional hepatic structures. In an article by Wu et al. [81], a hybrid bioink of cellulose nanocrystals and alginate was developed that demonstrated an excellent shear thinning property. The hybrid bioink can be extruded easily through a nozzle of 100 μm diameter without clogging. The ink was used to print a co-culture construct of hepatic cells and fibroblasts. Wang and colleagues [82] reported optimization of different printing parameters viz. polymer concentration, nozzle speed and extrusion rate for PLGA-based 3D printed scaffolds. Liver structures with desired wall thickness and contouring were then printed. Though the study showed promising results with quality of the 3D construct, they were not validated by its performance and compatibility with cells.

Table 2. Summary of major studies on 3D hepatic bioprinting in the last 5 years.

S. No.	Ink Composition	Cell/s Used	Bioprinting Process	Printed Structure/s	Application	Major Finding/s	References
1.	Liver dECM ¹ -gelatin	NIH3T3, HUVEC	Inkjet-based	2D and 3D liver shaped structures	Artificial tissue/organ regeneration	dECM powder-based bioink with enhanced printability and mechanical properties	[34]
2.	Pluronic F127-Alginate	HepG2/C3A	Extrusion-based	3D squared structure	In vitromodel for drug screening	3D hepatic model bioprinted without instructive signals	[78]
3.	Gelatin	Huh7	Extrusion-based	3D mesh with different strut angles	In vitrohepatic model with enhanced functionality	Scaffolds with strut angle of 60° showed increased hepatic functions	[79]
4.	PCL ² -Liver dECM; collagen	HepG2, BMMSCs	Extrusion-based	2D and 3D patterns	Hepatic tissue engineering	Bioink printing structures with optimum strength and differentiation capacity	[80]

Table 2. Cont.

S. No.	Ink Composition	Cell/s Used	Bioprinting Process	Printed Structure/s	Application	Major Finding/s	References
5.	Alginate-cellulose nanocrystals	Fibroblasts, human hepatoma cells	Extrusion-based	3D honeycomb structure	Hepatic tissue engineering	Novel cellulose-based bioink with excellent printability	[81]
6.	PLGA ³	Acellular	Extrusion-based	Single channel cubical; cylindrical; branched tri-channel hemisphere	Liver regenerative scaffolds	PLGA multichannel scaffolds using low-temperature deposition manufacturing device	[82]
7.	Gelatin-alginate	Primary hepatocellular carcinoma cells	Extrusion-based	3D cube	Personalized medicine	3D printed primary cells cultured in vitro with preservation of tumorigenicity	[83]
8.	gelatin-alginate-Matrigel™	Primary intrahepatic cholangiocarcinoma cells	Extrusion-based	3D cube	Personalized medicine	Patient-specific 3D bioprinted model for anticancer drug testing	[84]
9.	GelMA ⁴	HepG2/C3A spheroids	Inkjet-based	Liquid droplet	Organ-on-a-chip	Hepatic spheroid laden bioink printed directly in bioreactor culture chamber	[85]
10.	Collagen I-hyaluronan	Lx2, primary fetal activated hepatic stellate cells	Extrusion-based	Four-spoke wheel structure	In vitro drug screening, disease modeling	Tunable bioink with ability to incorporate other components for additional functionality	[86]
11.	Alginate-Cellulose nanocrystal-GelMA	NIH3T3, HepG2	Extrusion-based	3D honeycomb structure	Hepatic tissue engineering	Bicellular liver lobule-mimetic structures with precise positioning of the two cells	[87]
12.	Liver dECM-GelMA	Human-induced hepatocytes	Digital light processing	Inner gear-like structure	Liver substitute	Novel bioink compatible with high resolution digital light processing printing	[88]
13.	Collagen	Human adipose-derived stem cells (hASCs)	Extrusion-based	3D cube	Bioartificial liver	hASC-induced hepatocyte-like cells interfere with liver regeneration	[89]
14.	Alginate	Mouse primary hepatocytes, mesenchymal stem cells	Extrusion-based	3D cube	Hepatic tissue engineering	Co-culture of hepatic and stem cells in 3D bioprinted construct	[90]
15.	Alginate	Mouse-induced hepatocytes	Extrusion-based	3D cube	Bioartificial organs	Mouse-induced hepatocytes as hepatic cell source	[91]
16.	Galactosylated alginate	Mouse primary hepatocytes	Inkjet-based	Gel sheet	Hepatic tissue engineering	Controlled 3D geometrical arrangement of cells during printing	[92]
17.	Alginate	Mouse primary hepatocytes	Extrusion-based	3D cube	Hepatic tissue engineering	Long-term viability and functionality of primary hepatocytes	[93]
18.	Alginate	HepG2	Extrusion-based	3D cube	Regenerative medicine	Improved hepatic functions of HepG2	[94]
19.	Atelocollagen	Rat primary hepatocytes, HUVEC, human lung fibroblast	Extrusion-based	3D cube	Regenerative medicine	Co-culture of parenchymal and non-parenchymal cells, angiogenesis	[95]

Table 2. Cont.

S. No.	Ink Composition	Cell/s Used	Bioprinting Process	Printed Structure/s	Application	Major Finding/s	References
20.	Liver dECM-GelMA	HepLL, Caki-1	Lithography	Microfluidic device	Tumor progression model	Metastasis-on-a-chip for migration of kidney cancer cells to liver	[96]
21.	Human lung dECM-alginate-gelatin	HepaRG	Extrusion-based	3D cube	Infection and transduction studies	Printed tissue model allowed for extensive transduction otherwise not achieved in spheroid models	[97]
22.	NovoGel®	Primary cryopreserved human hepatocytes, hepatic stellate cells, HUVEC	Extrusion-based	Two-compartment planar geometry	In vitro hepatic model	Precise delivery of each cell type to designated locations, recapitulation of native tissue structure	[98]

¹ dECM: decellularized extracellular matrix; ² PCL: polycaprolactone; ³ PLGA: poly(lactic-co-glycolic acid); ⁴ GelMA: gelatin methacrylate.

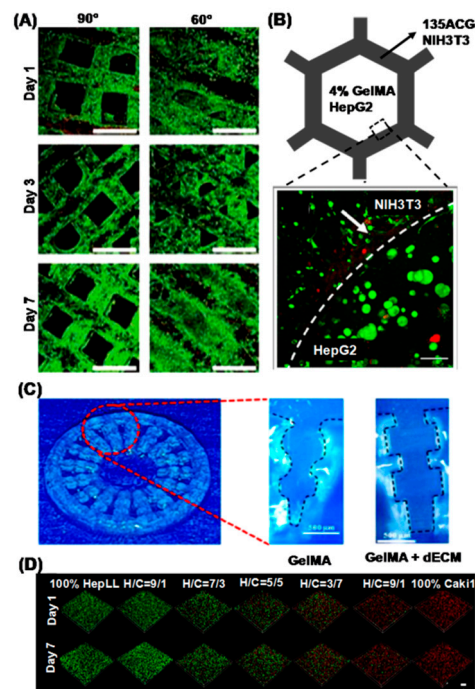


Figure 4. Three-dimensional hepatic printing with polymeric bioinks. (A) Confocal images of live/dead (green/red) staining of Huh7 cell seeded structures of different angles over 7 days (Magnification: 10 X; Scale bar: 500 μ m). Image reproduced with permission from [79]. (B) Adjacent NIH/3T3 in 1% alginate, 3% nanocrystalline cellulose and 5% GelMA (135ACG) and HepG2 in 4% GelMA on day 7 (green: live cells; red: dead cells; Scale bar: 100 μ m) Image reproduced with permission from [87]. (C) The macroscopic images of the digital light process printed GelMA/dECM and GelMA scaffolds in inner gear-like design (Scale bar: 500 μ m). Image reproduced with permission from [88]. (D) Confocal images of liver (HepLL) and kidney (Caki-1) cells co-cultured on metastasis-on-a-chip on day 1 and day 7 (Scale bar: 100 μ m). Image reproduced with permission from [96].

The major in vitro application of tissue engineered liver constructs is in drug discovery studies, whose paradigm is now shifting towards the development of personalized medicine and dose regimes. Individual/patient-specific cells are now being employed to generate 3D printed hepatic structures using polymeric bioinks for such studies. In a recent study by Xie et al. [83], hepatocellular carcinoma cells were isolated from differ-

ent patients, and long-term culture was established by bioprinting using gelatin-alginate inks. The bioprinted structures maintained the features of respective patients such as the genetic alterations and expression profile, thereby providing an excellent *in vitro* drug screening model for personalized medicine. In another study, primary intrahepatic cholangiocarcinoma cells were obtained from patients and printed in a grid architecture using gelatin–alginate–Matrigel™ composite hydrogel bioink. Studies on invasive and metastatic characteristics as well as response to anticancer drugs exhibited promising results for the development of personalized medicine [84]. A perfusion bioreactor interfaced with a bioprinter was used to print liver-on-a-chip using HepG2/C3A spheroid laden GelMA bioink. The platform showed enhanced liver specific functionalities and gene expression with drug response comparable to *in vivo* animal studies [85]. A collagen I-hyaluronic acid hybrid bioink was used to establish co-culture of primary human hepatocytes and liver stellate cells. The construct exhibited prolonged culture duration, enhanced albumin secretion and urea synthesis as well as altered response to acetaminophen. The simple platform could be very useful for the development of personalized medicine and dosage regimes, but it has to be validated further [86].

Another important application of 3D printed hepatic structures is in regenerative medicine. In the case of severe liver damage, external intervention is required for its regeneration. Either an *ex situ* bioartificial liver support device can be provided to carry out hepatic functions till the liver is regenerating, or *in vivo* implantation of a tissue engineered liver structure can be performed. Very recently, a hybrid 3D printed hepatic structure allowing the co-culture of fibroblast and hepatocytes was developed using alginate, nanocrystalline cellulose and GelMA. Mouse embryo fibroblast (NIH/3T3) was laden on a blended bioink of 1% alginate, 3% nanocrystalline cellulose and 5% GelMA (135ACG) that generated a stiff matrix. HepG2 was laden on 4% GelMA that engendered a soft matrix. The cell laden bioinks were then used to print a hepatic lobule-like structure. NIH/3T3 and HepG2 spheroids were confined to their respective spaces, thereby maintaining both homotypic and heterotypic interactions (Figure 4B). The hepatic cells exhibited arrest in proliferation with enhanced liver functionality [87]. In a recent study, a GelMA-dECM polymer blend was used to print hepatic structure using a digital light process based on a bioprinting device. Human-induced hepatocytes (HiHep) were added to GelMA and porcine dECM blend to constitute cell laden bioink that was printed into liver microtissue with an inner gear-like structure and a high surface area for cellular activities. The dECM improved the printability of the bioink and also enhanced cell viability and functionality as measured by albumin synthesis and blood urea nitrogen secretion (Figure 4C). Though only *in vitro* studies were carried out, the printed hepatic structure exhibited promising results to be employed as a liver substitute in hepatic regenerative medicine [88]. In one study, hepatic blocks were created by 3D printing of human adipose cells with collagen I bioink (later crosslinked by genpin) and differentiated to hepatocyte-like cells. Upon implantation in a rat induced for acute liver failure, the cells dislodged from the printed structure and translocated to hepatic portal veins after 4 weeks. The rat was also found to be recovering from liver failure as assessed by increased liver-specific parameters in the serum. The developed model exhibited to be a potential alternative to bioartificial liver models [89]. Another study by Kim and colleagues [90] reported the use of alginate bioink to print primary hepatocytes and mesenchymal stem cells (MSCs) for prolonged culture and enhanced hepatic functionality (albumin secretion and urea synthesis) and drug metabolic activity. The paracrine molecules secreted by MSCs indeed ameliorated the liver functions, and the 3D printed structure exhibited less hypoxic stress as compared to spheroids/organoids, while the tissue engineered platform needs to be validated further for its applications in drug screening or regenerative medicine. In a study by Kang et al. [91], mouse-induced hepatocyte-like cells (miHeps) were printed with alginate bioink, cultured *in vitro* for a week and then implanted *in vivo* in a mice liver damage model where it exhibited restoration of liver functions. In an interesting approach, Arai et al. [92] exhibited the use of galactosylated-alginate bioink to maintain the polarity of printed primary

hepatocytes. Performances of primary hepatocytes and HepG2 cells printed with alginate bioink or co-culture of hepatocytes, human umbilical vein endothelial cells and human lung fibroblasts bioprinted with collagen ink in a PCL framework were also reported by multiple studies [93–95]. All of them showed a prolonged survival and enhanced hepatic characteristics; however, the constructs need to be validated in terms of their applications.

Disease modeling is also among the important applications of hepatic tissue engineering, and 3D bioprinting has been already utilized in this field. A metastasis-on-a-chip model was developed to study the progression of kidney cancer to liver using dECM-GelMA-based printed microtissue (Figure 3D). The platform could be very useful to predict the dosage of anticancer drug at different stages of tumor progression [96]. In another instance, a viral infection model was developed by printing HepaRG cells in alginate-gelatin-dECMbioink. The addition of human dECM greatly enhanced the printability of the cell laden bioink and the hepatic functionality of HepaRG cells. The bioprinted hepatic structure was successfully developed and infected by human adenovirus 5 as well as a target gene, cyclophilin B, which was efficiently silenced by RNA interference upon transduction by adeno associated virus. Therefore, the developed structure served as a dual platform to study virus infection as well as virus-mediated gene therapy [97]. A liver fibrosis model by compound-induced liver injury was developed by bioprinting both parenchymal (hepatocytes) and non-parenchymal (endothelial cells and hepatic stellate cells). The bioprinted tissue showed excellent resemblance with native liver. Repeated, low-concentration exposure to methotrexate and thioacetamide led to the detection of hepatocellular damage, progressive fibrosis by formation of fibrillar collagens in patterns analogous to clinical fibrotic samples. The printed construct exhibited an excellent capacity to provide a platform for studying the mechanism of progression of liver injury and compound risk assessment [98].

5. Perspectives and Conclusions

Three-dimensional bioprinting has become crucial for developing tissue engineering constructs. The use of polymers in 3D printing has been beneficial to control the mechanical properties and stiffness of the printed structure as well as led to fabrication of live structures by allowing the preparation of cell laden bioinks. This has provided a huge advantage in developing soft tissues with low stiffness such as liver. Additionally, the precise positioning and delivery of bioink have made it possible to near-replicate the complex and detailed structure of liver, constituting different cells and ECM components. Of the different polymers, natural polymers provide many advantages for fabricating tissue engineered structures owing to their inherent property of biocompatibility. Of the many polymers, gelatin and decellularized matrices have been widely used to print 3D hepatic structures. The myriad of cells and ECM components present in the native structure of an organ poses extreme challenges in recapitulation of the structure. A limitation is also presented by the choice of biomaterial. Almost none of the polymers provide all the desired properties, such as mechanical strength, cytoadherence and ability to support and enhance functions of different cell types. This has been, however, overcome to some extent by using blends and composites of different polymers and other types of biomaterials. Still, printing the intricacies of tissue, especially in terms of resolution, remains an obstacle. As shown in Table 2, most of the bioprinted structures have a 3D cube shape and geometry, which is perhaps one of the simplest structures that can be 3D printed. Some studies have also reported bioprinting of the 3D hepatic lobule mimetic hexagonal structure; one of the studies actually printed a 3D liver shaped structure, which can be considered as an achievement [34]. It is also apparent that the most commonly used printing method is extrusion-based. Other 3D printing methods such as stereolithography and laser-assisted printing can also be explored to handle high viscosity bioink and high cell density, simultaneously improving the spatial resolution. Different types of cells and their sources also restrict the usage of 3D bioprinting to its full potential. The studies discussed in Section 4 suggest that employment

of multiple cell types is limited mainly to hepatic carcinoma, endothelial and fibroblast cells. More liver cells are needed to be incorporated further.

The studies systematized in this article indicate that polymeric bioinks have been mainly employed for two purposes viz. to enhance the stability of the printed hepatic structures and to fabricate hepatic structures for various tissue engineering applications. Though much success has been achieved in printing stable and durable structures, more research and development are required to print the detailed structure of the liver with defined spaces for ECM components and cells promoting homo- and heterotypic cell–cell and cell–ECM interactions. Tissue engineering applications mainly include in vitro drug screening and disease models as well as regenerative medicine with ex situ bioartificial liver support and in vivo implantable constructs. In all of these cases, the paradigm is now shifting towards the usage of individual/patient-specific cells so as to generate personalized tissue engineered constructs. This could prove to be very beneficial, particularly in developing personalized medicines and dosage regimes, avoid eliciting immune responses and circumventing graft rejection. However, cell sources still pose a major obstacle in such applications. More attention must now be diverted in printing stem cells and their differentiation towards hepatic lineage.

Author Contributions: J.S. conceived and designed the article, collected the reported studies/literature, wrote the article and prepared the figures. S.C.K. contributed in designing, literature survey, writing of the article and preparation of figures. N.C.K. contributed in writing 3D printing techniques and preparation of Figures 1 and 2. All authors have read and agreed to the published version of the manuscript.

Funding: This research received no external funding.

Institutional Review Board Statement: Not Applicable.

Informed Consent Statement: Not Applicable.

Data Availability Statement: No new data were created or analyzed in this study. Data sharing is not applicable to this article.

Conflicts of Interest: The authors declare no conflict of interest.

References

1. LeCluyse, E.L.; Witek, R.P.; Andersen, M.E.; Powers, M.J. Organotypic Liver Culture Models: Meeting Current Challenges in Toxicity Testing. *Crit. Rev. Toxicol.* **2012**, *42*, 501–548. [[CrossRef](#)]
2. Wells, R.G. Cellular Sources of Extracellular Matrix in Hepatic Fibrosis. *Clin. Liver Dis.* **2008**, *12*, 759–768. [[CrossRef](#)] [[PubMed](#)]
3. Elvevold, K.; Smedsrød, B.; Martinez, I. The Liver Sinusoidal Endothelial Cell: A Cell Type of Controversial and Confusing Identity. *Am. J. Physiol. Gastrointest. Liver Physiol.* **2008**, *294*, G391–G400. [[CrossRef](#)]
4. Friedman, S.L. Hepatic Stellate Cells: Protean, Multifunctional, and Enigmatic Cells of the Liver. *Physiol. Rev.* **2008**, *88*, 125–172. [[CrossRef](#)] [[PubMed](#)]
5. Kolios, G.; Valatas, V.; Kouroumalis, E. Role of Kupffer Cells in the Pathogenesis of Liver Disease. *World J. Gastroenterol.* **2006**, *12*, 7413–7420. [[CrossRef](#)]
6. Bogert, P.T.; LaRusso, N.F. Cholangiocyte Biology. *Curr. Opin. Gastroenterol.* **2007**, *23*, 299–305. [[CrossRef](#)]
7. Turner, R.; Lozoya, O.; Wang, Y.; Cardinale, V.; Gaudio, E.; Alpini, G.; Mendel, G.; Wauthier, E.; Barbier, C.; Alvaro, D.; et al. Human Hepatic Stem Cell and Maturational Liver Lineage Biology. *Hepatology* **2011**, *53*, 1035–1045. [[CrossRef](#)]
8. Sarkar, J.; Kamble, S.C.; Patil, R.; Kumar, A.; Gosavi, S.W. Gelatin Interpenetration in Poly N-isopropylacrylamide Network Reduces the Compressive Modulus of the Scaffold: A Property Employed to Mimic Hepatic Matrix Stiffness. *Biotechnol. Bioeng.* **2020**, *117*, 567–579. [[CrossRef](#)]
9. Wu, D.B.; Chen, E.Q.; Tang, H. Stem Cell Transplantation for the Treatment of End-Stage Liver Disease. *World J. Hepatol.* **2018**, *10*, 907–910. [[CrossRef](#)]
10. Kaplowitz, N. Idiosyncratic Drug Hepatotoxicity. *Nat. Rev. Drug Discov.* **2005**, *4*, 489–499. [[CrossRef](#)]
11. Lauschke, V.M.; Hendriks, D.F.G.; Bell, C.C.; Andersson, T.B.; Ingelman-Sundberg, M. Novel 3D Culture Systems for Studies of Human Liver Function and Assessments of the Hepatotoxicity of Drugs and Drug Candidates. *Chem. Res. Toxicol.* **2016**, *29*, 1936–1955. [[CrossRef](#)] [[PubMed](#)]
12. Hull, C.W. Apparatus for Production of Three-Dimensional Objects by Stereolithography. U.S. Patent 4575330A, 11 March 1986.
13. Kryou, C.; Leva, V.; Chatzipetrou, M.; Zergioti, I. Bioprinting for Liver Transplantation. *Bioengineering* **2019**, *6*, 95. [[CrossRef](#)] [[PubMed](#)]

14. Derakhshanfar, S.; Mbeleck, R.; Xu, K.; Zhang, X.; Zhong, W.; Xing, M. 3D Bioprinting for Biomedical Devices and Tissue Engineering: A Review of Recent Trends and Advances. *Bioact. Mater.* **2018**, *3*, 144–156. [[CrossRef](#)] [[PubMed](#)]
15. Murphy, S.V.; Atala, A. 3D Bioprinting of Tissues and Organs. *Nat. Biotechnol.* **2014**, *32*, 773–785. [[CrossRef](#)]
16. Munaz, A.; Vadivelu, R.K.; St. John, J.; Barton, M.; Kamble, H.; Nguyen, N.T. Three-Dimensional Printing of Biological Matters. *J. Sci. Adv. Mater. Devices* **2016**, *1*, 1–17. [[CrossRef](#)]
17. Tamay, D.G.; Usal, T.D.; Alagoz, A.S.; Yucel, D.; Hasirci, N.; Hasirci, V. 3D and 4D Printing of Polymers for Tissue Engineering Applications. *Front. Bioeng. Biotechnol.* **2019**, *7*, 164. [[CrossRef](#)]
18. Loai, S.; Kingston, B.R.; Wang, Z.; Philpott, D.N.; Tao, M.; Chen, H.-L.M. Clinical Perspectives on 3D Bioprinting Paradigms for Regenerative Medicine. *Regen. Med. Front.* **2019**, *1*, e190004.
19. Kolesky, D.B.; Homan, K.A.; Skylar-Scott, M.A.; Lewis, J.A. Three-Dimensional Bioprinting of Thick Vascularized Tissues. *Proc. Natl. Acad. Sci. USA* **2016**, *113*, 3179–3184. [[CrossRef](#)]
20. Kolesky, D.B.; Homan, K.A.; Skylar-Scott, M.; Lewis, J.A. In Vitro Human Tissues via Multi-Material 3-D Bioprinting. *Altern. Lab. Anim.* **2018**, *46*, 209–215. [[CrossRef](#)]
21. Ozbolat, I.T.; Hospodiuk, M. Current Advances and Future Perspectives in Extrusion-Based Bioprinting. *Biomaterials* **2016**, *76*, 321–343. [[CrossRef](#)]
22. Mandrycky, C.; Wang, Z.; Kim, K.; Kim, D.H. 3D Bioprinting for Engineering Complex Tissues. *Biotechnol. Adv.* **2016**, *34*, 422–434. [[CrossRef](#)] [[PubMed](#)]
23. Xu, T.; Jin, J.; Gregory, C.; Hickman, J.J.; Boland, T. Inkjet Printing of Viable Mammalian Cells. *Biomaterials* **2005**, *26*, 93–99. [[CrossRef](#)] [[PubMed](#)]
24. Boland, T.; Xu, T.; Damon, B.; Cui, X. Application of Inkjet Printing to Tissue Engineering. *Biotechnol. J.* **2006**, *1*, 910–917. [[CrossRef](#)] [[PubMed](#)]
25. Roth, E.A.; Xu, T.; Das, M.; Gregory, C.; Hickman, J.J.; Boland, T. Inkjet Printing for High-Throughput Cell Patterning. *Biomaterials* **2004**, *25*, 3707–3715. [[CrossRef](#)]
26. Pepper, M.E.; Seshadri, V.; Burg, T.C.; Burg, K.J.L.; Groff, R.E. Characterizing the Effects of Cell Settling on Bioprinter Output. *Biofabrication* **2012**, *4*, 011001. [[CrossRef](#)] [[PubMed](#)]
27. Guillemot, F.; Souquet, A.; Catros, S.; Guillotin, B.; Lopez, J.; Faucon, M.; Pippenger, B.; Bareille, R.; Rémy, M.; Bellance, S.; et al. High-Throughput Laser Printing of Cells and Biomaterials for Tissue Engineering. *Acta Biomater.* **2010**, *6*, 2494–2500. [[CrossRef](#)]
28. Wang, Z.; Abdulla, R.; Parker, B.; Samanipour, R.; Ghosh, S.; Kim, K. A Simple and High-Resolution Stereolithography-Based 3D Bioprinting System using Visible Light Crosslinkable Bioinks. *Biofabrication* **2015**, *7*, 045009. [[CrossRef](#)]
29. Wang, Z.; Kumar, H.; Tian, Z.; Jin, X.; Holzman, J.F.; Menard, F.; Kim, K. Visible Light Photoinitiation of Cell-Adhesive Gelatin Methacryloyl Hydrogels for Stereolithography 3D Bioprinting. *ACS Appl. Mater. Interfaces* **2018**, *10*, 26859–26869. [[CrossRef](#)]
30. Wang, X. Advanced Polymers for Three-Dimensional (3D) Organ Bioprinting. *Micromachines* **2019**, *10*, 814. [[CrossRef](#)]
31. Liu, F.; Chen, Q.; Liu, C.; Ao, Q.; Tian, X.; Fan, J.; Tong, H.; Wang, X. Natural Polymers for Organ 3D Bioprinting. *Polymers* **2018**, *10*, 1278. [[CrossRef](#)]
32. Chung, J.H.Y.; Naficy, S.; Yue, Z.; Kapsa, R.; Quigley, A.; Moulton, S.E.; Wallace, G.G. Bio-Ink Properties and Printability for Extrusion Printing Living Cells. *Biomater. Sci.* **2013**, *1*, 763–773. [[CrossRef](#)] [[PubMed](#)]
33. Jia, J.; Richards, D.J.; Pollard, S.; Tan, Y.; Rodriguez, J.; Visconti, R.P.; Trusk, T.C.; Yost, M.J.; Yao, H.; Markwald, R.R.; et al. Engineering Alginate as Bioink for Bioprinting. *Acta Biomater.* **2014**, *10*, 4323–4331. [[CrossRef](#)]
34. Kim, M.K.; Jeong, W.; Lee, S.M.; Kim, J.B.; Jin, S.; Kang, H.W. Decellularized Extracellular Matrix-Based Bio-Ink with Enhanced 3D Printability and Mechanical Properties. *Biofabrication* **2020**, *12*, 025003. [[CrossRef](#)]
35. Gaetani, R.; Doevendans, P.A.; Metz, C.H.G.; Alblas, J.; Messina, E.; Giacomello, A.; Sluijter, J.P.G. Cardiac Tissue Engineering Using Tissue Printing Technology and Human Cardiac Progenitor Cells. *Biomaterials* **2012**, *33*, 1782–1790. [[CrossRef](#)] [[PubMed](#)]
36. Melchels, F.P.W.; Feijen, J.; Grijpma, D.W. A Review on Stereolithography and Its Applications in Biomedical Engineering. *Biomaterials* **2010**, *31*, 6121–6130. [[CrossRef](#)] [[PubMed](#)]
37. Fan, R.; Piou, M.; Darling, E.; Cormier, D.; Sun, J.; Wan, J. Bio-Printing Cell-Laden Matrigel-Agarose Constructs. *J. Biomater. Appl.* **2016**, *31*, 684–692. [[CrossRef](#)] [[PubMed](#)]
38. Lee, D.Y.; Lee, H.; Kim, Y.; Yoo, S.Y.; Chung, W.J.; Kim, G. Phage as Versatile Nanoink for Printing 3-D Cell-Laden Scaffolds. *Acta Biomater.* **2016**, *29*, 112–124. [[CrossRef](#)]
39. Liu, F.; Liu, C.; Chen, Q.; Ao, Q.; Tian, X.; Fan, J.; Tong, H.; Wang, X. Progress in Organ 3D Bioprinting. *Int. J. Bioprinting* **2018**, *4*, 128. [[CrossRef](#)]
40. Panwar, A.; Tan, L.P. Current Status of Bioinks for Micro-Extrusion-Based 3D Bioprinting. *Molecules* **2016**, *21*, 685. [[CrossRef](#)]
41. Blaeser, A.; Duarte Campos, D.F.; Puster, U.; Richtering, W.; Stevens, M.M.; Fischer, H. Controlling Shear Stress in 3D Bioprinting is a Key Factor to Balance Printing Resolution and Stem Cell Integrity. *Adv. Healthc. Mater.* **2016**, *5*, 326–333. [[CrossRef](#)]
42. Causa, F.; Sarracino, F.; De Santis, R.; Netti, P.A.; Ambrosio, L.; Nicolais, L. Basic Structural Parameters for the Design of Composite Structures as Ligament Augmentation Devices. *J. Appl. Biomater. Biomech.* **2006**, *4*, 21–30. [[PubMed](#)]
43. Hospodiuk, M.; Dey, M.; Sosnoski, D.; Ozbolat, I.T. The Bioink: A Comprehensive Review on Bioprintable Materials. *Biotechnol. Adv.* **2017**, *35*, 217–239. [[CrossRef](#)]
44. Gopinathan, J.; Noh, I. Recent Trends in Bioinks for 3D Printing. *Biomater. Res.* **2018**, *22*, 11. [[CrossRef](#)] [[PubMed](#)]

45. Colosi, C.; Shin, S.R.; Manoharan, V.; Massa, S.; Costantini, M.; Barbetta, A.; Dokmeci, M.R.; Dentini, M.; Khademhosseini, A. Microfluidic Bioprinting of Heterogeneous 3D Tissue Constructs Using Low-Viscosity Bioink. *Adv. Mater.* **2016**, *28*, 677–684. [[CrossRef](#)]
46. Wang, X.; Yu, X.; Yan, Y.; Zhang, R. Liver Tissue Responses To gelatin and Gelatin/Chitosan Gels. *J. Biomed. Mater. Res. Part A* **2008**, *87*, 62–68. [[CrossRef](#)] [[PubMed](#)]
47. Gaetani, R.; Feyen, D.A.M.; Verhage, V.; Slaats, R.; Messina, E.; Christman, K.L.; Giacomello, A.; Doevendans, P.A.F.M.; Sluijter, J.P.G. Epicardial Application of Cardiac Progenitor Cells in a 3D-Printed Gelatin/Hyaluronic Acid Patch Preserves Cardiac Function after Myocardial Infarction. *Biomaterials* **2015**, *61*, 339–348. [[CrossRef](#)]
48. Xiao, W.; He, J.; Nichol, J.W.; Wang, L.; Hutson, C.B.; Wang, B.; Du, Y.; Fan, H.; Khademhosseini, A. Synthesis and Characterization of Photocrosslinkable Gelatin and Silk Fibroin Interpenetrating Polymer Network Hydrogels. *Acta Biomater.* **2011**, *7*, 2384–2393. [[CrossRef](#)]
49. Kang, H.W.; Lee, S.J.; Ko, I.K.; Kengla, C.; Yoo, J.J.; Atala, A. A 3D Bioprinting System to Produce Human-Scale Tissue Constructs with Structural Integrity. *Nat. Biotechnol.* **2016**, *34*, 312–319. [[CrossRef](#)]
50. Lee, H.; Cho, D.W. One-Step Fabrication of an Organ-on-a-Chip with Spatial Heterogeneity Using a 3D Bioprinting Technology. *Lab Chip* **2016**, *16*, 2618–2625. [[CrossRef](#)]
51. Gauvin, R.; Chen, Y.C.; Lee, J.W.; Soman, P.; Zorlutuna, P.; Nichol, J.W.; Bae, H.; Chen, S.; Khademhosseini, A. Microfabrication of Complex Porous Tissue Engineering Scaffolds Using 3D Projection Stereolithography. *Biomaterials* **2012**, *33*, 3824–3834. [[CrossRef](#)]
52. Wang, X. Bioartificial Organ Manufacturing Technologies. *Cell Transplant.* **2019**, *28*, 5–17. [[CrossRef](#)] [[PubMed](#)]
53. Yue, K.; Trujillo-de Santiago, G.; Alvarez, M.M.; Tamayol, A.; Annabi, N.; Khademhosseini, A. Synthesis, Properties, and Biomedical Applications of Gelatin Methacryloyl (GelMA) Hydrogels. *Biomaterials* **2015**, *73*, 254–271. [[CrossRef](#)] [[PubMed](#)]
54. Stanton, M.M.; Samitier, J.; Sánchez, S. Bioprinting of 3D Hydrogels. *Lab Chip* **2015**, *15*, 3111–3115. [[CrossRef](#)]
55. Lee, K.Y.; Mooney, D.J. Alginate: Properties and Biomedical Applications. *Prog. Polym. Sci.* **2012**, *37*, 106–126. [[CrossRef](#)] [[PubMed](#)]
56. Pawar, S.N.; Edgar, K.J. Alginate Derivatization: A Review of Chemistry, Properties and Applications. *Biomaterials* **2012**, *33*, 3279–3305. [[CrossRef](#)]
57. Axpe, E.; Oyen, M. Applications of Alginate-Based Bioinks in 3D Bioprinting. *Int. J. Mol. Sci.* **2016**, *17*, 1976. [[CrossRef](#)]
58. Daly, A.C.; Cunniffe, G.M.; Sathy, B.N.; Jeon, O.; Alsborg, E.; Kelly, D.J. 3D Bioprinting of Developmentally Inspired Templates for Whole Bone Organ Engineering. *Adv. Healthc. Mater.* **2016**, *5*, 2353–2362. [[CrossRef](#)]
59. Choi, Y.J.; Yi, H.G.; Kim, S.W.; Cho, D.W. 3D Cell Printed Tissue Analogues: A New Platform for Theranostics. *Theranostics* **2017**, *7*, 3118–3137. [[CrossRef](#)]
60. Mao, B.; Divoux, T.; Snabre, P. Impact of Saccharides on the Drying Kinetics of Agarose Gels Measured by In-Situ Interferometry. *Sci. Rep.* **2017**, *7*, 41185. [[CrossRef](#)]
61. Zucca, P.; Fernandez-Lafuente, R.; Sanjust, E. Agarose and Its Derivatives as Supports for Enzyme Immobilization. *Molecules* **2016**, *21*, 1577. [[CrossRef](#)]
62. Kreimendahl, F.; Köpf, M.; Thiebes, A.L.; Duarte Campos, D.F.; Blaeser, A.; Schmitz-Rode, T.; Apel, C.; Jockenhoevel, S.; Fischer, H. Three-Dimensional Printing and Angiogenesis: Tailored Agarose-Type i Collagen Blends Comprise Three-Dimensional Printability and Angiogenesis Potential for Tissue-Engineered Substitutes. *Tissue Eng. Part C Methods* **2017**, *23*, 604–615. [[CrossRef](#)] [[PubMed](#)]
63. Yang, X.; Lu, Z.; Wu, H.; Li, W.; Zheng, L.; Zhao, J. Collagen-Alginate as Bioink for Three-Dimensional (3D) Cell Printing Based Cartilage Tissue Engineering. *Mater. Sci. Eng. C* **2018**, *83*, 195–201. [[CrossRef](#)] [[PubMed](#)]
64. Rodriguez-Pascual, F.; Slatter, D.A. Collagen Cross-Linking: Insights on the Evolution of Metazoan Extracellular Matrix. *Sci. Rep.* **2016**, *6*, 37374. [[CrossRef](#)] [[PubMed](#)]
65. Stratesteffen, H.; Köpf, M.; Kreimendahl, F.; Blaeser, A.; Jockenhoevel, S.; Fischer, H. GelMA-Collagen Blends Enable Drop-on-Demand 3D Printability and Promote Angiogenesis. *Biofabrication* **2017**, *9*, 045002. [[CrossRef](#)]
66. Law, N.; Doney, B.; Glover, H.; Qin, Y.; Aman, Z.M.; Sercombe, T.B.; Liew, L.J.; Dilley, R.J.; Doyle, B.J. Characterisation of Hyaluronic Acid Methylcellulose Hydrogels for 3D Bioprinting. *J. Mech. Behav. Biomed. Mater.* **2018**, *77*, 389–399. [[CrossRef](#)]
67. Martínez Ávila, H.; Schwarz, S.; Rotter, N.; Gatenholm, P. 3D Bioprinting of Human Chondrocyte-Laden Nanocellulose Hydrogels for Patient-Specific Auricular Cartilage Regeneration. *Bioprinting* **2016**, *1–2*, 22–35.
68. Müller, M.; Öztürk, E.; Arlov, Ø.; Gatenholm, P.; Zenobi-Wong, M. Alginate Sulfate–Nanocellulose Bioinks for Cartilage Bioprinting Applications. *Ann. Biomed. Eng.* **2017**, *45*, 210–223. [[CrossRef](#)]
69. Markstedt, K.; Escalante, A.; Toriz, G.; Gatenholm, P. Biomimetic Inks Based on Cellulose Nanofibrils and Cross-Linkable Xylans for 3D Printing. *ACS Appl. Mater. Interfaces* **2017**, *9*, 40878–40886. [[CrossRef](#)]
70. Bedossa, P.; Paradis, V. Liver Extracellular Matrix in Health and Disease. *J. Pathol.* **2003**, *200*, 504–515. [[CrossRef](#)]
71. Dzobo, K.; Motaung, K.S.C.M.; Adesida, A. Recent Trends in Decellularized Extracellular Matrix Bioinks for 3D Printing: An Updated Review. *Int. J. Mol. Sci.* **2019**, *20*, 4628. [[CrossRef](#)]
72. Pepelanova, I.; Kruppa, K.; Scheper, T.; Lavrentieva, A. Gelatin-methacryloyl (GelMA) Hydrogels with Defined Degree of Functionalization as a Versatile Toolkit for 3D Cell Culture and Extrusion Bioprinting. *Bioengineering* **2018**, *5*, 55. [[CrossRef](#)]
73. Park, J.; Lee, S.J.; Chung, S.; Lee, J.H.; Kim, W.D.; Lee, J.Y.; Park, S.A. Cell-Laden 3D Bioprinting Hydrogel Matrix Depending on Different Compositions for Soft Tissue Engineering: Characterization and Evaluation. *Mater. Sci. Eng. C* **2017**, *71*, 678–684. [[CrossRef](#)] [[PubMed](#)]

74. Pati, F.; Jang, J.; Ha, D.H.; Won Kim, S.; Rhie, J.W.; Shim, J.H.; Kim, D.H.; Cho, D.W. Printing Three-Dimensional Tissue Analogues with Decellularized Extracellular Matrix Bioink. *Nat. Commun.* **2014**, *5*, 3935. [[CrossRef](#)] [[PubMed](#)]
75. Jang, J.; Kim, T.G.; Kim, B.S.; Kim, S.W.; Kwon, S.M.; Cho, D.W. Tailoring Mechanical Properties of Decellularized Extracellular Matrix Bioink by Vitamin B2-Induced Photo-Crosslinking. *Acta Biomater.* **2016**, *33*, 88–95. [[CrossRef](#)] [[PubMed](#)]
76. Jang, J.; Park, H.J.; Kim, S.W.; Kim, H.; Park, J.Y.; Na, S.J.; Kim, H.J.; Park, M.N.; Choi, S.H.; Park, S.H.; et al. 3D Printed Complex Tissue Construct Using Stem Cell-Laden Decellularized Extracellular Matrix Bioinks for Cardiac Repair. *Biomaterials* **2017**, *112*, 264–274. [[CrossRef](#)]
77. Pati, F.; Ha, D.H.; Jang, J.; Han, H.H.; Rhie, J.W.; Cho, D.W. Biomimetic 3D Tissue Printing for Soft Tissue Regeneration. *Biomaterials* **2015**, *62*, 164–175. [[CrossRef](#)]
78. Gori, M.; Giannitelli, S.M.; Torre, M.; Mozetic, P.; Abbruzzese, F.; Trombetta, M.; Traversa, E.; Moroni, L.; Rainer, A. Biofabrication of Hepatic Constructs by 3D Bioprinting of a Cell-Laden Thermogel: An Effective Tool to Assess Drug-Induced Hepatotoxic Response. *Adv. Healthc. Mater.* **2020**, *9*, e2001163. [[CrossRef](#)]
79. Lewis, P.L.; Green, R.M.; Shah, R.N. 3D-Printed Gelatin Scaffolds of Differing Pore Geometry Modulate Hepatocyte Function and Gene Expression. *Acta Biomater.* **2018**, *69*, 63–70. [[CrossRef](#)]
80. Lee, H.; Han, W.; Kim, H.; Ha, D.H.; Jang, J.; Kim, B.S.; Cho, D.W. Development of Liver Decellularized Extracellular Matrix Bioink for Three-Dimensional Cell Printing-Based Liver Tissue Engineering. *Biomacromolecules* **2017**, *18*, 1229–1237. [[CrossRef](#)]
81. Wu, Y.; Lin, Z.Y.; Wenger, A.C.; Tam, K.C.; Tang, X.S. 3D Bioprinting of Liver-Mimetic Construct with Alginate/Cellulose Nanocrystal Hybrid Bioink. *Bioprinting* **2018**, *9*, 1–6. [[CrossRef](#)]
82. Wang, X.; Rijff, B.L.; Khang, G. A Building-Block Approach to 3D Printing a Multichannel, Organ-Regenerative Scaffold. *J. Tissue Eng. Regen. Med.* **2017**, *11*, 1403–1411. [[CrossRef](#)] [[PubMed](#)]
83. Xie, F.; Sun, L.; Pang, Y.; Xu, G.; Jin, B.; Xu, H.; Lu, X.; Xu, Y.; Du, S.; Wang, Y.; et al. Three-Dimensional bio-Printing of Primary Human Hepatocellular Carcinoma for Personalized Medicine. *Biomaterials* **2021**, *265*, 120416. [[CrossRef](#)] [[PubMed](#)]
84. Mao, S.; He, J.; Zhao, Y.; Liu, T.; Xie, F.; Yang, H.; Mao, Y.; Pang, Y.; Sun, W. Bioprinting of Patient-Derived In Vitro Intrahepatic Cholangiocarcinoma Tumor Model: Establishment, Evaluation and Anti-Cancer Drug Testing. *Biofabrication* **2020**, *12*, 045014. [[CrossRef](#)] [[PubMed](#)]
85. Bhise, N.S.; Manoharan, V.; Massa, S.; Tamayol, A.; Ghaderi, M.; Miscuglio, M.; Lang, Q.; Zhang, Y.S.; Shin, S.R.; Calzone, G.; et al. A Liver-on-a-Chip Platform with Bioprinted Hepatic Spheroids. *Biofabrication* **2016**, *8*, 014101. [[CrossRef](#)] [[PubMed](#)]
86. Mazzocchi, A.; Devarasetty, M.; Huntwork, R.; Soker, S.; Skardal, A. Optimization of Collagen Type I-Hyaluronan Hybrid Bioink for 3D Bioprinted Liver Microenvironments. *Biofabrication* **2019**, *11*, 015003. [[CrossRef](#)]
87. Wu, Y.; Wenger, A.; Golzar, H.; Tang, X.S. 3D Bioprinting of Bicellular Liver Lobule-Mimetic Structures via Microextrusion of Cellulose Nanocrystal-Incorporated Shear-Thinning Bioink. *Sci. Rep.* **2020**, *10*, 20648. [[CrossRef](#)]
88. Mao, Q.; Wang, Y.; Li, Y.; Juengpanich, S.; Li, W.; Chen, M.; Yin, J.; Fu, J.; Cai, X. Fabrication of Liver Microtissue with Liver Decellularized Extracellular Matrix (dECM) Bioink by Digital Light Processing (DLP) Bioprinting. *Mater. Sci. Eng. C* **2020**, *109*, 110625. [[CrossRef](#)]
89. Lee, J.S.; Yoon, H.; Yoon, D.; Kim, G.H.; Yang, H.T.; Chun, W. Development of Hepatic Blocks Using Human Adipose Tissue-Derived Stem Cells Through Three-Dimensional Cell Printing Techniques. *J. Mater. Chem. B* **2017**, *5*, 1098–1107. [[CrossRef](#)]
90. Kim, Y.; Kang, K.; Yoon, S.; Kim, J.S.; Park, S.A.; Kim, W.D.; Lee, S.B.; Ryu, K.Y.; Jeong, J.; Choi, D. Prolongation of Liver-Specific Function for Primary Hepatocytes Maintenance in 3D Printed Architectures. *Organogenesis* **2018**, *14*, 1–12. [[CrossRef](#)]
91. Kang, K.; Kim, Y.; Jeon, H.; Lee, S.B.; Kim, J.S.; Park, S.A.; Kim, W.D.; Yang, H.M.; Kim, S.J.; Jeong, J.; et al. Three-Dimensional Bioprinting of Hepatic Structures with Directly Converted Hepatocyte-Like Cells. *Tissue Eng. Part A* **2018**, *24*, 576–583. [[CrossRef](#)]
92. Arai, K.; Yoshida, T.; Okabe, M.; Goto, M.; Mir, T.A.; Soko, C.; Tsukamoto, Y.; Akaike, T.; Nikaide, T.; Zhou, K.; et al. Fabrication of 3D-Culture Platform with Sandwich Architecture for Preserving Liver-Specific Functions of Hepatocytes Using 3D Bioprinter. *J. Biomed. Mater. Res. Part A* **2017**, *105*, 1583–1592. [[CrossRef](#)] [[PubMed](#)]
93. Kim, Y.; Kang, K.; Jeong, J.; Paik, S.S.; Kim, J.S.; Park, S.A.; Kim, W.D.; Park, J.; Choi, D. Three-Dimensional (3D) Printing of Mouse Primary Hepatocytes to Generate 3D Hepatic Structure. *Ann. Surg. Treat. Res.* **2017**, *92*, 67–72. [[CrossRef](#)] [[PubMed](#)]
94. Jeon, H.; Kang, K.; Park, S.A.; Kim, W.D.; Paik, S.S.; Lee, S.H.; Jeong, J.; Choi, D. Generation of Multilayered 3D Structures of HepG2 Cells Using a Bio-Printing Technique. *Gut Liver* **2017**, *11*, 121–128. [[CrossRef](#)] [[PubMed](#)]
95. Lee, J.W.; Choi, Y.J.; Yong, W.J.; Pati, F.; Shim, J.H.; Kang, K.S.; Kang, I.H.; Park, J.; Cho, D.W. Development of a 3D Cell Printed Construct Considering Angiogenesis for Liver Tissue Engineering. *Biofabrication* **2016**, *8*, 015007. [[CrossRef](#)] [[PubMed](#)]
96. Wang, Y.; Wu, D.; Wu, G.; Wu, J.; Lu, S.; Lo, J.; He, Y.; Zhao, C.; Zhao, X.; Zhang, H.; et al. Metastasis-on-a-Chip Mimicking the Progression of Kidney Cancer in the Liver for Predicting Treatment Efficacy. *Theranostics* **2020**, *10*, 300–311. [[CrossRef](#)] [[PubMed](#)]
97. Hiller, T.; Berg, J.; Elomaa, L.; Röhrs, V.; Ullah, I.; Schaar, K.; Dietrich, A.C.; Al-Zeer, M.A.; Kurtz, A.; Hocke, A.C.; et al. Generation of a 3D Liver Model Comprising Human Extracellular Matrix in an Alginate/Gelatin-Based Bioink by Extrusion Bioprinting for Infection and Transduction Studies. *Int. J. Mol. Sci.* **2018**, *19*, 3129. [[CrossRef](#)]
98. Norona, L.M.; Nguyen, D.G.; Gerber, D.A.; Presnell, S.C.; LeCluyse, E.L. Modeling Compound-Induced Fibrogenesis In Vitro Using Three-Dimensional Bioprinted Human Liver Tissues. *Toxicol. Sci.* **2016**, *154*, 354–367. [[CrossRef](#)]